Calcium signaling in chemorepellant Slit2-dependent regulation of neuronal migration

Hua-tai Xu, Xiao-bing Yuan, Chen-bing Guan, Shumin Duan, Chien-ping Wu, and Linyin Feng*

Institute of Neuroscience, Shanghai Institutes for Biological Sciences, Chinese Academy of Sciences, 320 Yueyang Road, Shanghai 200031, China

Edited by Lynn T. Landmesser, Case Western Reserve University, Cleveland, OH, and approved January 20, 2004 (received for review June 24, 2003)

Migration of neuronal precursor cells in the developing brain is guided by extracellular cues, but intracellular signaling processes underlying the guidance of neuronal migration are largely unknown. By examining the migration of cerebellar granule neurons along the surface of cocultured astroglial cells, we found that an extracellular gradient of Slit2, a chemorepellant for neuronal migration *in vivo*, caused a reversal in the direction of migration without affecting the migration speed. A Slit2 gradient elevated the intracellular concentration of Ca^{2+}, probably due to calcium release from the internal store, led to a reversal of the preexisting asymmetric intracellular Ca^{2+} distribution in the soma of migrating neurons, and this reversal was closely related with its action of reversing the migrating direction. Asymmetric Ca^{2+} distribution in the soma was both necessary and sufficient for directing neuronal migration. These results have demonstrated an important role for Ca^{2+} in mediating neuronal responses to Slit2 and suggest a general mechanism for neuronal guidance.

In the developing nervous system, a large number of neuronal precursor cells migrate from the site of birth to their destination along the surface of radial glial cells (1–3). Recent studies (4–6) have shown that several secreted or cell-surface proteins, including the netrins, Slits, and the Semaphorins can function as guidance cues for directing neuronal migration. However, most studies were performed on explants of brain tissue, and intracellular mechanisms mediating neuronal responses to these guidance cues are still poorly understood. Calcium signaling is known to be involved in regulating neuronal migration. In cultured explants of cerebellar tissue, granule cell migration correlates with intracellular Ca^{2+} fluctuations and blockade of Ca^{2+} influx retards migration (7–9). Voltage-gated Ca^{2+} channels are essential for postembryonic neuronal migration in *Caenorhabditis elegans* (10). Slit2 is a well known secreted chemorepellant for migration of many types of neurons in the CNS (11–13). In the present study, the action of Slit2 on single-neuron migration *in vitro* was examined, and the role of calcium signal in mediating the repulsive action of Slit2 was explored. By using a cell culture model of migration of cerebellar granule cells on cocultured radial glial cells, we found that a gradient of Slit2 in front of the migrating neuron caused a reversal of the direction of migration without significantly affecting the subsequent migratory speed. We also found that a Slit2-induced Ca^{2+} signaling appeared to mediate the repulsive action on neuronal migration, and that Ca^{2+} release from intracellular store through inositol trisphosphate receptor channels played a major role in the Ca^{2+} signaling.

Materials and Methods

Coculture of Cells. The methods of coculturing granular cells and astroglia cells were similar to that described by Hatten (14). In short, astroglial cells from the cerebellum of P0-P3 SD rats isolated with a step gradient (35%/65%) of Percoll were plated on a polylysine-coated glass coverslip. Purified neurons were added 1 day later. The cells were cultured with Basal Medium Eagle (GIBCO) supplemented with 10% horse serum (GIBCO), glucose (6 mM), and glutamine (4 mM) in 5% CO_2 and 95% humidity air incubator.

Labeling with 1,1′-Dioctadecyl-3,3,3′,3′-tetramethylindocarbocyanine. To label granule cells in the coculture preparation, granule cell suspension was first incubated with 1,1′-dioctadecyl-3,3,3′,3′-tetramethylindocarbocyanine (3.5 μg/ml) for 30 min, and was then centrifuged and washed three times. The labeled granule cells were then added to the astroglia culture. After 24–48 h, the fluorescent migrating granule cells were studied under a Leica DMR fluorescence microscope equipped with Leica lens 506148 and cool charge-coupled device camera (Spot System, Chinetek Scientific, Hong Kong).

Application of Guidance Cues. A glass pipette with a tip opening of $\approx$1 μm was placed at 15 μm perpendicular to the long process of an astroglial cell and 100 μM apart from the center of the cell soma of a granule cell, which was attached on its long process. A standard pressure pulse of 3 psi (1 psi = 6.89 kPa) in amplitude and 20 ms in duration, generated by a pulse generator, was applied to the pipette at a frequency of 2 Hz. Images of the migrating neuron were recorded by time-lapse video microscopy by means of an Olympus CK-40 phase contrast microscope and were stored in a PC computer for further analysis.

Preparation of Slit2. Slit2 was purified from the conditioned medium collected from a cultured HEK cell line (provided by Y. Rao, Department of Anatomy and Neurobiology, Washington University, St. Louis) which stably expressed human Slit2-myc. The conditioned medium was collected within 24 h after confluence. The pH value of the conditioned medium was adjusted to 5.5 with acetic acid and then the medium was loaded to an SP fast flow column prebalanced with 1× PBS (pH 5.5). After washing with three bed volumes of 1× PBS (pH 5.5), the proteins were eluted with gradients of NaCl solution from 0 to 1 M in 10 bed volume. The fractions from 0.4 to 1 M NaCl solutions were collected and their pH value was adjusted to 7.5. Positive fractions were identified with Western blot, and were then desalted and were concentrated with ultrafiltration (100 kDa).

Calcium Imaging. To observe the intracellular calcium concentration, two Ca^{2+} indicator dyes, Fluo-4/Fura-red AM (Molecular Probes), dissolved in 0.0125% pluronic acid and diluted with DMSO (6 and 8 μM for growth cone staining and 3 and 4 μM for soma staining, respectively), were loaded into the cells. The surplus serum was removed by rinsing three times with L15 medium at 37°C before loading dyes. The cells were rinsed three times again with L15 medium 30 min after loading to remove the surplus Fluo-4/Fura-red AM. The labeled cells were then hatched in L15 medium for 25 min. A Zeiss LSM-510 confocal microscope with a 488-nm wavelength light from an argon laser was used to examine the intracellular Ca^{2+}. Fluorescence images for ratiometric Ca^{2+} were collected at 505- to 550-nm and $\geq$585-nm wavelengths, for Fluo-4

This paper was submitted directly (Track II) to the PNAS office.

Abbreviations: IP, immunoprecipitated; BAPTA-AM, 1,2-bis(2-aminophenoxy)ethane-*N*,*N*,*N*′,*N*′-tetraacetic acid, tetra (acetoxymethyl) ester; $[Ca^{2+}]i$, intracellular Ca^{2+} concentration.

*To whom correspondence should be addressed. E-mail: lyfeng@ion.ac.cn.

www.pnas.org/cgi/doi/10.1073/pnas.0303893101

and Furo-red, respectively, by using 512 pixel box and a 20× Fluor (NA1.2) objective. For all experiments, the laser power was attenuated by using neutral density filters to 1–10% of the maximum. Fluorescence images were collected every 0.5–1 min, the intensity of fluorescence was quantified, and changes were normalized to baseline by using Zeiss LSM-510 software.

Normalization of Net and Total Migration Distances. Refer to the schematic diagram, Fig. 3*C Inset*, for the definitions of D1–D4. The normalized net migration distance of a granule cell is defined as the ratio of its net migration distance during the first 20 min following the onset of extracellular gradient (between t = 0 min and t = 20 min, *Inset*, D2) to its net migration distance in the 20-min control period (between $t = -20$ min and $t = 0$ min, D1), that is, D2/D1. D2 is defined as negative when the value of net migration distance at t = 20 min was smaller than that at t = 0 min. The normalized total migration distance is defined as the ratio of D3 (the largest value of net migration distance from t = 0 min, *Inset*) plus D4 (the net migration distance between the largest value and that of t = 20 min) to D1; i.e., $(|D3| + |D4|)/D1$.

Asymmetric Index of Intracellular Calcium Distribution. Asymmetric indices are calculated to quantify the asymmetry of calcium distribution in the cell body of neurons. To perform these calculations, the cell body of a neuron is divided into six segments (F1–F6) along its long axis, and the asymmetric index is calculated with an equation of $(F1 - F6)/(F1 + F6)$, where F1 and F6 are mean intensities of Fluo-4/Fura-red ratio fluorescence at the front and rear end of the cell body, respectively.

Results

Astroglia and granule neurons obtained from the cerebellum of postnatal rats were cocultured (14). Within 48 h after plating purified granule cells onto cultures of purified astroglia, many neurons were found to attach to astroglia and were migrating along the elongated astroglial processes. The migrating neuron, together with its leading and trailing processes, could be visualized by staining the granule cells with 1,1′-dioctadecyl-3,3,3′,3′-tetramethylindocarbocyanine before the plating (Fig. 1*A*). To examine the effect of extracellular guidance cues on neuronal migration, we applied a microscopic gradient of the cues in front or at the rear of the migrating neuron by repetitive puffing of solutions containing the cue through a micropipette placed at a distance of 100 μm from the soma (Fig. 1 *B* and *C* and refs. 15 and 16), and the direction and speed of migration was monitored by measuring the position of the soma.

In the first set of experiments, we examined the effect of Slit2. The migration of granule cell on the surface of an elongated astroglial cell was first monitored for a control period. A microscopic gradient of the purified myc-tagged Slit2 was then applied in front of the granule cell. As illustrated in Fig. 2*A Left*, within minutes after the onset of the Slit2 gradient, the forward migration of the granule cell was halted and then the direction of migration was reversed. In control experiments, in which the Slit2-myc in the micropipette solution had been immunoprecipitated (IP) with anti-myc antibody before the experiment, the forward movement was found largely unaffected (Fig. 2*A Right*).

The results from experiments using normal Slit2-myc solution and Slit2-IP solution in the pipette are summarized in Fig. 2*B*. It can be seen in Fig. 2*B* that migration of granule neurons on cocultured astroglial cells usually proceeded in a saltatory manner, with stationary and migratory phases as well as occasional reversal in the direction, even in the absence of any extracellular cues (17). Despite the saltatory manner of migration, there was apparent reversal of the direction of migration in the presence of Slit2-myc gradient in the majority of neurons examined, whereas no significant effect on the forward migration was detected in control experiments.

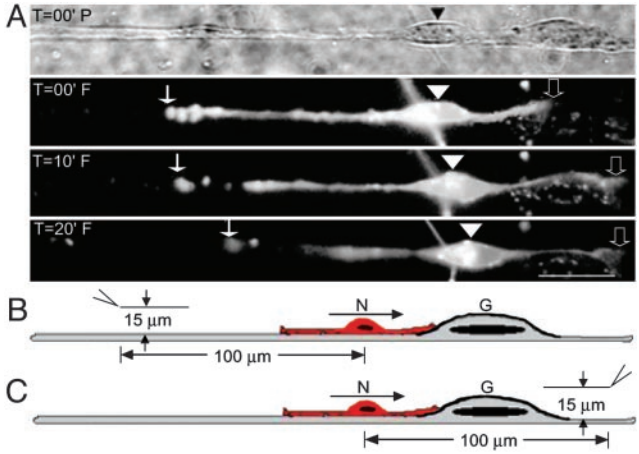

Fig. 1. Single-neuron migration and experimental preparations. (*A*) A 1,1′-dioctadecyl-3,3,3′,3′-tetramethylindocarbocyanine-labeled cerebellar granule neuron migrating on an astroglial cell. The first image is a microscopic photo taken in bright field, and the next three images were taken under fluorescence microscopy. Migration of the entire neuron (cell body, leading and trailing process, marked by triangles, empty arrows, and arrows, respectively) can be seen over the 20-min period of observation. (Scale bar, 20 μM.) (*B* and *C*) Schematic diagrams depicting positions of the micropipette used for delivering guidance cues at the front (*C*) and at the rear (*B*) of the migrating neuron, respectively. G, astroglial cell; N, granule cell. Horizontal arrow above the soma indicates the direction of migration.

To quantify the effect of guidance cue on migration of each neuron, we measured the net distance of soma translocation during the 20-min control period (D1) and the first 20 min after the onset of the gradient (D2). The net translocation in the presence of the gradient of guidance cue was normalized by that of the control period (D2/D1) and was plotted in the cumulative

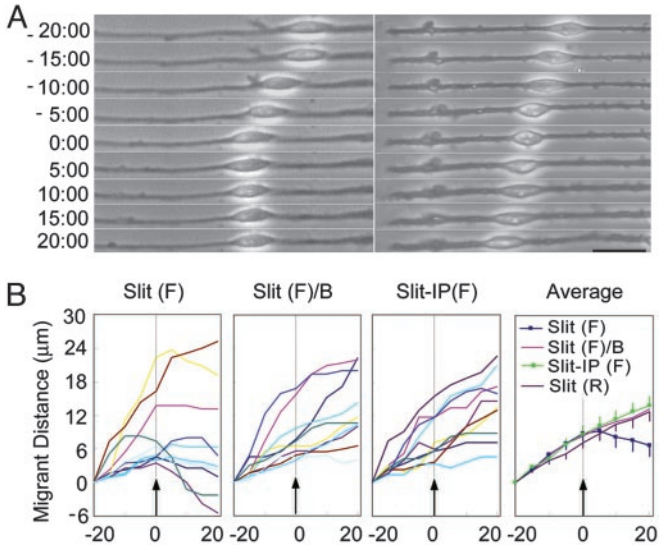

Fig. 2. Regulation of granule cell migration by Slit2. (*A Left*) Sequential images of a migrating granule cell taken at 5-min intervals during the control period (−20 to 0 min) and after application of Slit2-myc (8 ng/μl in the pipette) gradient in front of the neuron (0–20 min). (*Right*) Images of another granule cell under an IP-Slit2-myc gradient. (Bar, 20 μm.) (*B*) In each of the three images from the left, migrating paths of 10 migrating granule cells before and after front-end application (at time 0) of Slit2-myc gradient, Slit2-myc with 25 μM BAPTA-AM in the culture medium, and IP-Slit2-myc are plotted, respectively. The averaged paths are shown on the right. Each data point represents mean ± SEM (n = 10).

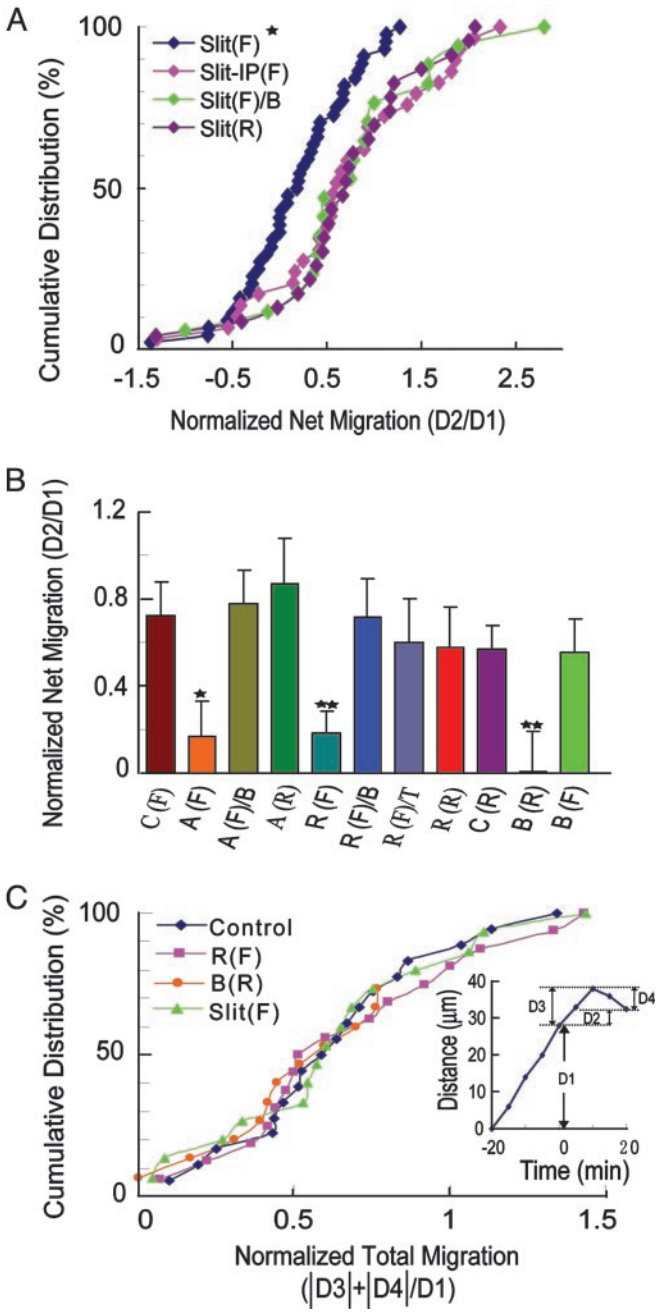

Fig. 3. Net and total migration distances of granule cells. (*A*) Cumulative distribution of normalized net migration distances. Each point represents the result from one neuron. The abscissa is the normalized net migration distance of the neuron (D2/D1, for definitions see Fig. 3*C Inset*), and the ordinate is the percentage of neurons in the same treatment group that had equal or lower normalized net migration distances. Slit (F), front-end application of Slit2-myc gradient ($n = 24$); Slit-IP(F), front-end application of Slit2-myc immunoprecipitated with anti-myc antibody ($n = 29$); Slit (F)/B, front-end application of Slit2-myc with BAPTA-AM in the culture medium ($n = 17$); and Slit(R), rear-end application of Slit2-myc gradient ($n = 23$). The distribution of Slit(F) group is significantly different from the other three groups ($P < 0.05$, Kolmogorov–Smirnov test). (*B*) A histogram showing the averaged normalized net migration distances of neurons in different treatment groups. C(F), front-end application of culture medium (control group, $n = 29$); A(F), front-end application of acetycholine gradient (100 mM in the pipette, $n = 21$); A(F)/B, front-end application of acetycholine gradient with BAPTA-AM (10 μM) in culture medium ($n = 15$); A(R), rear-end application of acetycholine gradient ($n = 14$); R(F), front-end application of ryanodine gradient (1 μM in the pipette, $n = 31$); R(F)/B, front-end application of ryanodine gradient with BAPTA-AM in the bath ($n = 17$); R(F)/T, front-end application of ryanodine gradient with thapsigargin (1 μM) in the bath ($n = 30$); C(R), rear-end application of culture medium ($n = 25$); R(R), rear-end application of ryanodine gradient ($n = 22$); B(R), rear-end application of BAPTA-AM gradient (250 μM in the pipette, $n = 25$); and B(F), front-end application of BAPTA-AM gradient (250 μM in the pipette, $n = 14$). The averaged net migration distances of R(F), B(R) ($P < 0.01$), and A(F) ($P < 0.05$) groups are significantly smaller than those under other conditions (Kolmogorov–Smirnov test). (*C*) Cumulative distribution of normalized total migration distances [(|D3| + |D4|)/D1] in response to gradient of extracellular guidance cues. No significant difference in total migration distances could be seen between the control group and groups of front-end application of Slit2-myc or ryanodine and rear-end application of BAPTA-AM ($P > 0.05$, Kolmogorov–Smirnov test). (*Inset*) The schematic diagram shows the definitions of D1 to D4. For details of calculating normalized net and total migration distances, see *Materials and Methods*.

distribution graph shown in Fig. 3*A*. Statistical analysis of the distribution indicates significant shift in the migratory pattern of these neurons after front-end application of Slit2 gradient compared with the distribution of migratory control cells, the net distance of migration (D2/D1) under a Slit2 gradient was significantly smaller (Fig. 3*B*). Interestingly, we found that when the Slit2-myc gradient is applied at the rear of the migrating neuron, there was no apparent effect on neuronal migration (Fig. 3*A*). Repulsive signaling triggered by the Slit2 gradient at the rear of the neuron may be commensurate to the existing direction of the migrating neuron, thus causing no alteration in neuronal migration.

The Slit2 gradient reduced the net distance of migration, but does the gradient indeed change the speed of migration? To clarify this question, we analyzed the speed of migration by measuring the effects of gradients of Slit2, as well as of 1,2-bis(2-aminophenoxy)ethane-*N*,*N*,*N*′,*N*′-tetraacetic acid, tetra (acetoxymethyl) ester (BAPTA-AM) and ryanodine (see below), on the total rather than the net distance of translocation. When the normalized total migration distance [(|D3| + |D4|)/D1, depicted in Fig. 3*C Inset*] rather than the net migration distance (D2/D1) the neuron had made over the 20-min period after the onset of the gradients was calculated, we found no difference in the cumulative distribution patterns for migration under gradients of Slit2, BAPTA-AM, or ryanodine, as compared with the migration under control conditions (Fig. 3*C*). Thus, these extracellular guidance cues did not alter the overall migration speed of the granule cells.

To investigate the role of Ca^{2+} signaling in the neuronal migration, particularly its role in the repulsive action of Slit2 in cerebellar granule cells, we preincubated the culture with a membrane permeable Ca^{2+} chelator, BAPTA-AM (25 μM), which clamped the intracellular Ca^{2+} concentration ($[Ca^{2+}]i$) at a low level, we found that the repulsive action of Slit2 gradient on granule cell migration was abolished (second image of Figs. 2*B* and 3*A*). Thus, $[Ca^{2+}]i$ changes were necessary for Slit2-induced repulsive action on neuronal migration. However, does the Slit2 gradient indeed trigger $[Ca^{2+}]i$ change in these neurons? We have monitored $[Ca^{2+}]i$ by loading Ca^{2+}-sensitive fluorescent dye Furo-red (8 μM) and Fluo-4 (6 μM) into the granule cells. As mentioned above, in our experiments the majority of granule neurons were found migrated along the long processes of the cocultured astroglial cells. However, a certain percentage of granule neurons in the coculture did not migrate and they were thus named as stationary neurons. In the soma of migrating neuron, we consistently observed an asymmetric distribution of Ca^{2+} with $[Ca^{2+}]i$ higher in the rear end (see Movie 1, which is published as supporting information on the PNAS web site). By contrast, there was no apparent asymmetric distribution of $[Ca^{2+}]i$ in stationary neurons (see Movie 2, which is published as supporting information on the PNAS web site).

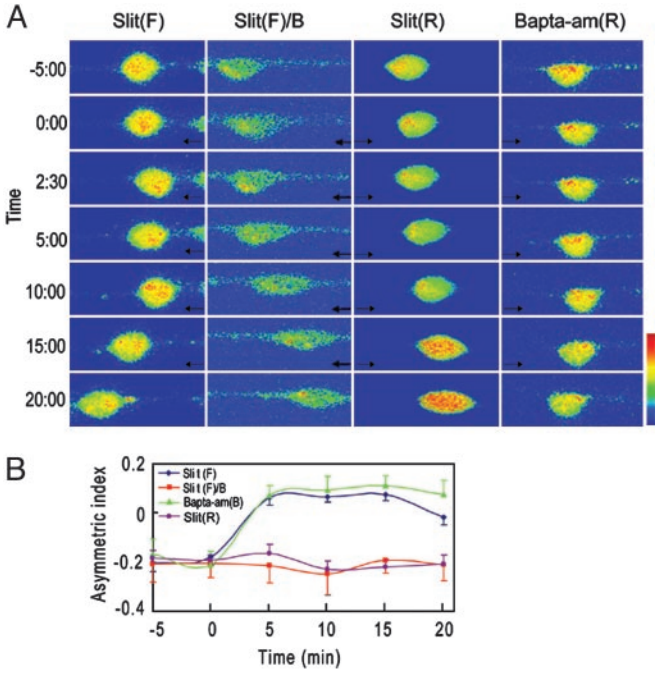

Fig. 4. Calcium signaling in migrating granule cell. (*A*) Calcium signals revealed by Fluo-4/Fura-red ratio fluorescence in four migrating neurons in response to application of Slit2 and BAPTA-AM gradient. Front-end application of Slit2 gradient reversed the direction of migration as well as the polarity of calcium distribution (*Left*). Front-end application of Slit2 gradient plus BAPTA-AM in the bath (25 μM, *Left Center*) and rear-end application of Slit2 gradient (*Right Center*) did not change the polarity of calcium distribution, nor did they reverse the direction of migration. Rear-end application of BAPTA-AM gradient reversed both the direction of migration and the polarity of calcium distribution (*Right*). Black arrows, application of Slit2 or BAPTA-AM gradient. (Scale bar, 10 μm.) The intensity of fluorescence is coded in the color bar on the right. (*B*) Asymmetric index (see *Materials and Methods*) of calcium distribution in migrating neurons. Front-end application of Slit2 gradient (blue curve, $n = 36$) or rear-end application of BAPTA-AM gradient (green curve, $n = 10$) changed the averaged asymmetric index from a negative value to positive, reflecting the reversal of polarity of calcium distribution, whereas no significant changes were seen after front-end application of Slit2 with BAPTA-AM in the bath (red curve, $n = 10$) or rear-end application of Slit2 gradient (purple curve, $n = 10$).

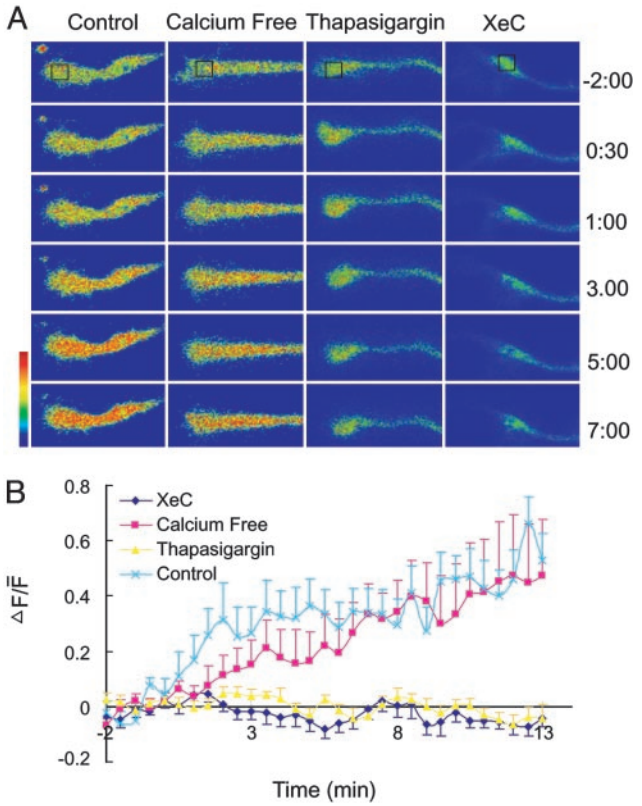

Fig. 5. Calcium elevation in the growth cones induced by Slit2 gradient. (*A*) Intracellular calcium level in the growth cones of granule cells revealed by Fluo-4/Fura-red ratio fluorescence at different times (min:sec) before and after the onset (at $t = 0{:}00$) of a Slit2 gradient. Front-end application of Slit2 gradient elevated $[Ca^{2+}]$i (*Left*). Slit2 gradient still elevated calcium level in the growth cone after the culture had been preincubated in Ca^{2+}-free medium supplemented with EGTA (2 mM, *Left Center*). Adding thapsigargin (1 μM, *Right Center*) or xestospongin C (XeC; 2 μM, *Right*) in the culture medium abolished the action of Slit2 gradient in elevating $[Ca^{2+}]$i. The intensity of fluorescence is coded in the pseudocolor bar at left, with red representing the highest intensities. (*B*) Curves showing the averaged normalized changes of $[Ca^{2+}]$i, expressed as percentage changes in Fluo-4/Fura-red fluorescence ($\Delta F/\bar{F}$) sampled from a representative area of the growth cones (areas within the black flames in *A*), induced by a Slit2 gradient (started at $t = 0$ min) in the normal culture medium (blue line, $n = 26$), in the calcium-free medium plus EGTA (red line, $n = 8$), in medium supplemented with thapsigargin (yellow line, $n = 9$), and in medium supplemented with XeC (dark blue line, $n = 18$), respectively.

When a gradient of Slit2 was applied in front of the migrating neuron, we observed a pronounced Ca^{2+} elevation at the front end of the soma. Interestingly, shortly after this elevation, the distribution of Ca^{2+} in the soma of a number of neurons underwent a period of dynamic changes with higher concentration at the front or/and at the rear end of the soma. Eventually, a steady state of higher concentration of Ca^{2+} at the front end of soma was reached, and the direction of migration was reversed accordingly. A typical example is shown in Fig. 4*A Left*. The averaged asymmetric indices shown in Fig. 4*B* also clearly revealed the reversal of Ca^{2+} distribution after application of Slit2 and BAPTA-AM gradients. Usually, this Ca^{2+} signal induced by a gradient of Slit2 disappeared within 10 min after the removal of the gradient. Thus, an asymmetric Ca^{2+} distribution with a higher concentration in the rear end correlated with forward migration of these neurons, and Slit2 not only induced an elevation of $[Ca^{2+}]$i but consequently reversed the Ca^{2+} distribution in the soma, resulting in a reversal in the direction of neuronal migration.

How did the Slit2 gradient induce the elevation of $[Ca^{2+}]$i in cultured granule neurons? In our experiments, we found that the elevation of $[Ca^{2+}]$i was induced both in the soma and in the growth cone of granule neurons by application of a Slit2 gradient. However, it was more marked in the growth cone than in the soma. Therefore, it was more convenient to do measurements in the growth cone and to study the underlying mechanisms. The elevation of $[Ca^{2+}]$i in a growth cone after application of a Slit2 gradient is shown in the first image of Fig. 5*A*. When we removed the extracellular calcium by adding EGTA (2 mM) to a calcium-free medium, the $[Ca^{2+}]$i in the growth cones was still elevated by application of a Slit2 gradient, as seen in Fig. 5. However, if the internal calcium store of the neuron was depleted with thapsigargin (1 μM), a Slit2 gradient no longer caused the elevation of $[Ca^{2+}]$i. Furthermore, application of the inhibitor of inositol trisphosphate receptor xestospongin C (2 μM), which prevented the release of Ca^{2+} from the internal calcium store, also abolished the Slit2-induced Ca^{2+} elevation (Fig. 5). Therefore, the intracellular calcium store and the inositol trisphosphate receptor play essential roles in mediating Slit2's action of elevating intracellular calcium concentration.

We showed that a Slit2 gradient caused a change in $[Ca^{2+}]$i distribution which seemed to be correlated with a directional reversal in neuronal migration. It is natural to ask whether

application of gradients of other substances that create asymmetric Ca^{2+} distribution in the granule cells would have the similar effect. We found that front application of a gradient of acetylcholine (100 mM in the pipette), which is known to elevate neuronal Ca^{2+} level by opening nicotinic channels, reversed the migration of granule cells on astroglial cells in a manner similar to that produced by front application of a Slit2 gradient (Fig. 3*B*). Front application of a gradient of ryanodine (1 μM in the pipette), a drug known to activate Ca^{2+} release channels on intracellular membranes at low concentration (18) and to trigger Ca^{2+} release from internal stores, also produced similar repulsive action on the migration of these neurons (Fig. 3*B*). That the ryanodine gradient indeed exerted its effect by releasing Ca^{2+} from internal stores was further confirmed by the finding that the repulsive effect of ryanodine was abolished when the cultures were preincubated with BAPTA-AM (25 μM) or thapsigargin (1 μM), which clamped $[Ca^{2+}]$i at a low level or depleted internal Ca^{2+} stores, respectively (Fig. 3*B*). Finally, we manipulated the $[Ca^{2+}]$i level directly by applying a gradient of BAPTA-AM to the migrating cell. Front application of BAPTA-AM gradient produced no effect on neuronal migration, whereas application of the same gradient at the rear retarded the forward migration (Fig. 3*B*). Fluorescence imaging of Ca^{2+} indicates that a reversed asymmetric Ca^{2+} distribution was induced by the rear-end BAPTA-AM gradient, with $[Ca^{2+}]$i higher at the end away from the pipette (Fig. 4*A*). Taken together, these results support the notion that front-end application of guidance signals that trigger, in various ways, a "front-high, rear-low" Ca^{2+} distribution would be sufficient to induce a reversal in the direction of neuronal migration, whereas guidance signals that trigger a "front-low, rear-high" distribution are commensurate with the existing Ca^{2+} distribution in the migrating neuron, and do not change the direction of migration.

Discussion

Calcium has been known to play important roles not only in migration of neurons but also in cell motility of many types of cell. For instance, it has been reported that a transient increase of Ca^{2+} occurred in migrating human neutrophils during chemokinesis, chemotaxis, and phagocytosis (19). Buffering of $[Ca^{2+}]$i or removal of extracellular Ca^{2+} blocked this transient and reduced or inhibited the migration of neurotrophils.

Consistent with what we found in the present study, asymmetric distribution of intracellular Ca^{2+} has been reported to be associated with migration of nonneuronal cells. A gradient with increasing Ca^{2+} from the front to the rear of migrating cells has been observed in eosinophils, fibroblasts, and *Dictyostelium*, when these cells maintained a specific direction of migration (20–22). The polarity of Ca^{2+} distribution in these migrating cells is similar to what we found in the migrating granule cell. Observations on neuronal growth cone migration showed that higher levels of $[Ca^{2+}]$i were found in growth cones of neuroblastoma cells that were not advancing (23). It was also reported that $[Ca^{2+}]$i spikes transiently inhibited growth cone migration of dorsal root ganglia neurons (24), and the rate of axon outgrowth *in vivo* was inversely proportional to the frequency of $[Ca^{2+}]$i transients (25).

The results in the present study indicate that calcium signal is involved in the repulsive action of the guidance cue Slit2. This notion is supported by the following evidence: (*i*) Application of a gradient of Slit2 resulted in an elevation of Ca^{2+} concentration in the growth cone. Furthermore, when Slit2 gradient was applied at the front of a migrating granule neuron, elevation of $[Ca^{2+}]$i occurred at the front end of soma, which consequently caused a reversal of the preexisting "front-lower, rear-higher" distribution of $[Ca^{2+}]$i; (*ii*) this reversal of Ca^{2+} distribution in the soma was found to be closely related with the reversal of migrating direction caused by a Slit2 gradient, which is commensurate with the observation in eosinophil that when the eosinophil turned, the region of the cell that became the new leading edge had the lowest $[Ca^{2+}]$i (20); (*iii*) bath application of BAPTA-AM or thapsigargin abolished the repulsive action of Slit2 and ryanodine gradients; and (*iv*) finally, front-end application of gradients of other substances that are known to elevate intracellular Ca^{2+} also had repulsive actions on granule neurons and, similarly, caused a reversal of Ca^{2+} distribution in the soma. It thus seems that repulsive guidance cues regulate the migrating direction by altering $[Ca^{2+}]$i distribution.

The mechanisms by which the Ca^{2+} elevation induced by Slit2 gradient caused a reversal of Ca^{2+} distribution across the cell body are not known. We found that the total level of intracellular concentration of calcium in the cell body was increased by $\approx$5% after applying a Slit2 gradient. The reversal of Ca^{2+} distribution could be due to the Ca^{2+} elevation at the front end of the soma induced by a front-end Slit2 gradient, but the possibility that Ca^{2+} concentration at the rear end was reduced simultaneously by some unknown mechanism cannot be excluded. In view of the observation that in many neurons a Slit2 gradient first induced dynamic changes of Ca^{2+} distribution before the final reversal of the original gradient of distribution, it seems that the redistribution of Ca^{2+} concentration is a complex process. In addition, some dynamic calcium "transients" that occurred at the frequency of once in several minutes were seen in a few neurons, however, we did not find significant causal relationship between these changes and the reversal of direction of migration. An example of such transients can be seen in Fig. 4*A Right Center*.

In the growth cone of cultured neurons, it is well documented that calcium is involved in mediating its responses to directional guidance cues (26–29). We also proved in the present study that an extracellular Slit2 gradient elevated $[Ca^{2+}]$i in the growth cone. However, it is not clear that when a granule neuron was attached to and migrating along the astroglial process, whether such a Ca^{2+} signal in the growth cone induced by Slit2 gradient was transferred to and caused a reversal of Ca^{2+} distribution in the soma, or, the reversal of Ca^{2+} distribution in the soma was directly induced by the Slit2 gradient itself.

We also do not know the mechanisms by which a redistribution of intracellular Ca^{2+} reversed the migrating direction of the neuron. It is generally believed that calcium plays roles in cell motility by way of its regulation on cytoskeleton and its associated proteins. However, the signaling cascades between Ca^{2+} concentration change and cytoskeleton reorganization in migrating neurons are poorly known. Changes in cytoskeletal organization and roles they may play in migration have been studied in cerebellar granule neurons (30, 31). Calcium transients were proved to regulate growth cone motility through the Ca^{2+}-dependent phosphatase calcineurin and the latter ultimately affects the growth cone actin cytoskeleton (32, 33). Recently it was reported that Ca^{2+} transients regulate the growth cone motility and guidance through activation of the protease calpain (29). The roles of these molecules in neuronal migration remain to be explored.

It is interesting that preincubation of cultures in calcium-free medium supplemented with EGTA did not prevent the $[Ca^{2+}]$i elevation in growth cones induced by Slit2, whereas application of xestospongin C in the medium did. We also found that bath application of 2-amino-5-phosphonovaleric acid, the antagonist of NMDA receptor, had no effect on elevation of $[Ca^{2+}]$i caused by the Slit2 gradient (results not shown). Thus, elevation of $[Ca^{2+}]$i induced by Slit2 was based on calcium release from internal calcium store by means of inositol trisphosphate channels rather than the calcium influx.

We thank Prof. Mu-ming Poo and Dr. Yi Rao for encouragement, discussion, and comments. This work was supported by National Key Project for Basic Research of China Grant G2000077800, Shanghai Science and Technology Commission Grants 00JC14019 and 018014015, and National Natural Science Foundation of China Grant 39920018.

1. Hatten, M. E. (1999) *Annu. Rev. Neurosci.* **22,** 511–539.
2. Goldowitz, D. & Hamre, K. (1998) *Trends Neurosci.* **21,** 375–382.
3. Parnavelas, J. G. (2000) *Trends Neurosci.* **23,** 126–131.
4. Eickholt, B. J., Mackenzie, S. L., Graham, A., Walsh, F. S. & Doherty, P. (1999) *Development (Cambridge, U.K.)* **126,** 2181–2189.
5. Anton, E. S., Marchionni, M. A., Lee, K. F. & Rakic, P. (1997) *Development (Cambridge, U.K.)* **124,** 3501–3510.
6. Alcantara, S., Ruiz, M., De Castro, F., Soriano, E. & Sotelo, C. (2000) *Development (Cambridge, U.K.)* **127,** 1359–1372.
7. Komuro, H. & Rakic, P. (1993) *Science* **260,** 95–97.
8. Komuro, H. & Rakic, P. (1996) *Neuron* **17,** 275–285.
9. Komuro, H. & Rakic, P. (1998) *J. Neurobiol.* **37,** 110–130.
10. Tam, T., Mathews, E., Snutch, T. P. & Schafer, W. R. (2000) *Dev. Biol.* **226,** 104–117.
11. Wu, W., Wong, K., Chen, J., Jiang, Z., Dupuis, S., Wu, J. Y. & Rao, Y. (1999) *Nature* **400,** 331–336.
12. Zhu, Y., Li, H., Zhou, L., Wu, J. Y. & Rao, Y. (1999) *Neuron* **23,** 473–485.
13. Brose, K., Bland, K. S., Wang, K. H., Arnott, D., Henzel, W., Goodman, C. S., Tessier-Lavigne, M. & Kidd, T. (1999) *Cell* **96,** 795–806.
14. Hatten, M. E. (1985) *J. Cell Biol.* **100,** 384–396.
15. Song, H.-J., Ming, G.-L. & Poo, M.-M. (1997) *Nature* **388,** 275–279.
16. Song, H., Ming, G., He, Z., Lehmann, M., McKerracher, L., Tessier-Lavigne, M. & Poo, M. (1998) *Science* **281,** 1515–1518.
17. Stitt, T. N., Gasser, U. E. & Hatten, M. E. (1991) *Ann. N.Y. Acad. Sci.* **633,** 113–121.
18. Zucchi, R. & Ronca-Testoni, S. (1997) *Pharmacol. Rev.* **49,** 1–51.
19. Marks, P. W. & Maxfield, F. R. (1990) *J. Cell Biol.* **110,** 43–52.
20. Brundage, R. A., Fogarty, K. E., Tuft, R. A. & Fay, F. S. (1991) *Science* **254,** 703–706.
21. Hahn, K., DeBiasio, R. & Taylor, D. L. (1992) *Nature* **359,** 736–738.
22. Yumura, S., Furuya, K. & Takeuchi, I. (1996) *J. Cell Sci.* **109,** 2673–2678.
23. Silver, R. A., Lamb, A. G. & Bolsover, S. R. (1989) *J. Neurosci.* **9,** 4007–4020.
24. Gomez, T. M., Snow, D. M. & Letourneau, P. C. (1995) *Neuron* **14,** 1233–1246.
25. Gomez, T. M. & Spitzer, N. C. (1999) *Nature* **397,** 350–355.
26. Hong, K., Nishiyama, M., Henley, J., Tessier-Lavigne, M. & Poo, M. (2000) *Nature* **403,** 93–98.
27. Zheng, J. Q. (2000) *Nature* **403,** 89–93.
28. Gomez, T. M., Robles, E., Poo, M. & Spitzer, N. C. (2001) *Science* **291,** 1983–1987.
29. Robles, E., Huttenlocher, A. & Gomez, T. M. (2003) *Neuron* **38,** 597–609.
30. Rivas, R. J. & Hatten, M. E. (1995) *J. Neurosci.* **15,** 981–989.
31. Rakic, P., Knyihar-Csillik, E. & Csillik, B. (1996) *Proc. Natl. Acad. Sci. USA* **93,** 9218–9222.
32. Lautermilch, N. J. & Spitzer, N. C. (2000) *J. Neurosci.* **20,** 315–325.
33. Spitzer, N. C., Lautermilch, N. J., Smith, R. D. & Gomez, T. M. (2000) *BioEssays* **22,** 811–817.